Reprint of the 7th AIAA/USAF/NASA/ISSMO Symposium on Multidisciplinary Analysis and Optimization, St. Louis, Sept. 15-18, 1998.
AIAA Paper 98-4828

Improvement of a Preliminary Design and Optimization Program for the Evaluation of Future Aircraft Projects

D. Strohmeyer and R. Seubert
Institute of Design Aerodynamics, DLR Brunswick, Germany

Nomenclature

A	=	aspect ratio
B	=	wing span
C_D	=	drag coefficient
$C_{D,0}$	=	zero-lift drag coefficient, C_D (C_L=0)
C_L	=	lift coefficient
C_L / C_D	=	lift-over-drag ratio, L / D
C_M	=	pitching moment coefficient
C_p	=	pressure coefficient
c	=	chord length
H	=	flight altitude, km
h	=	height, m
k	=	k-factor of quadratic drag polar
k_α	=	correction factor for vortex lift
l_μ	=	aerodynamic mean chord
M_∞	=	freestream Mach number
R	=	range, km
S	=	wing reference area, m^2
W	=	weight, t
x, y, z	=	cartesian coordinates
$x_{C.G.}$	=	x-position of the center of gravity
x_N	=	x-position of aerodynamic neutral point
α	=	angle of attack
ε	=	trim angle
φ_{25}	=	sweep angle of quarter-chord line
λ	=	bypass ratio
η	=	non-dimensionalized chord length
τ	=	taper ratio

Indices

C.G.	=	center of gravity
C	=	canard
cr	=	cruise
f	=	friction
HTP	=	horizontal tailplane
lin	=	linear
loc	=	local
max	=	maximum value
opt	=	optimum value
p	=	pressure
req	=	required

Introduction

Analyses of the international operating airlines predict an annual increase of the worldwide air traffic between 5 % and 7 % for the next decades (Fig. 1). Based on these predictions the large aircraft companies and national aeronautical research institutes think about alternative concepts such as the supersonic commercial transport aircraft (SCT) or the Megaliner (A3XX) - which go beyond the conventional stretching of the existing wide bodies (B747, A330/A340).

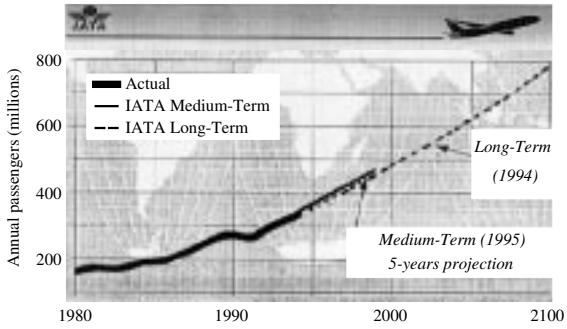

Fig. 1 IATA projection of world international scheduled passenger traffic.

At the Institute of Design Aerodynamics, DLR Brunswick, special attention is drawn to the evaluation of advanced technologies and unconventional concepts for the improvement of the aerodynamic efficiency of a Megaliner configuration. Within the project '3FF' (Three Surface Aircraft, TSA) the integration of a second lifting control device in the nose region, a so-called canard, is designed and its effects with respect to aerodynamics, flight control as well as aeroelastics studied. Further attention is drawn to the aerodynamic design and optimization of future SCT configurations and related problems.

In both cases, the final evaluation of the technologies and concepts is based on integrated predesign studies with an improved version of the **Pr**eliminary **D**esign and **O**ptimization **P**rogram PrADO,[1-3] originally developed at the Institute of Aircraft Design and Structure Mechanics of Technical University Braunschweig. For this purpose, the aerodynamics module of PrADO was improved by the implementation of the **Hi**gher-Order **S**ubsonic / **S**upersonic **S**ingularity Method HISSS,[4] provided by Daimler-Benz Aerospace (DASA), Munich. In addition the flight mechanics module of PrADO was extended to allow the simulation of trimed missions for TSA configurations. Finally, a model for current and future SCT engines[5] (e.g. mid-tandem fan) provided by the Institute of Propulsion Technology, DLR Cologne, was integrated into the predesign code.

It is the aim of this work-in-progress paper to show the present state of development, validation and calibration of PrADO, drawing special attention to the aerodynamic part of the design process, and discuss first preliminary results obtained for an SCT and Megaliner canard design.

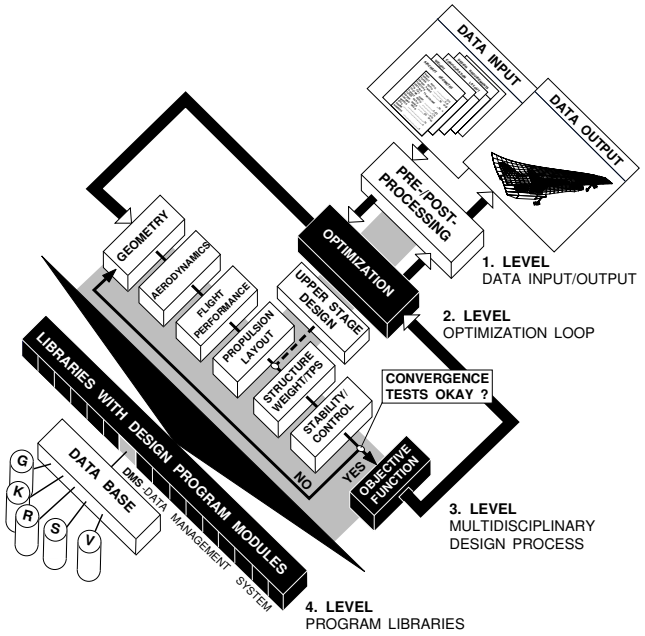

Fig. 2 Structure of the integrated aircraft design program PrADO.[3]

PrADO - Structure

The structure of the design code PrADO,[1-3] which has been used by university and industry for the assessment of various flight vehicle and engine related technologies and concepts, is subdivided into 4 levels as illustrated in Fig. 2 (including the option of the design of two-stage-to-orbit transportation system,[3] note the upper stage design):

1. Level: Data Input/Output. These routines are necessary for the data input of the user-specified baseline design (e.g. mission requirements and constraints). They build up a complete data base for the configuration necessary to start the design iteration. Missing values are provided by estimations from a statistical data processor. Fixed external data bases include material properties, engine performance and aerodynamic characteristics.

2. Level: Optimization Loop. Herein routines are included for the minimization of a given object function (e.g. take-off weight, fuel consumption, operating costs) varying free independent design parameters (e.g. cruise speed, range, aspect ratio). For the optimization the following methods are available: A modified version of Vanderplaats gradient method, a procedure of Jacob based on a search-direction strategy and an evolution method. Other programs within this level generate the design-specific object function and check the design constraints.

3. Level: Multidisciplinary Design Process. This level simulates the sequential interdisciplinary design process with the interactions between the involved disciplines (e.g. aerodynamics, flight performance, propulsion, structure mass, stability and control). This part of PrADO calls the analysis methods which define the physical relationship between the independent (e.g. payload, range, geometry assumption) and dependent variables (e.g. fuel weight, operational empty weight, max. take-off weight). For the exchange of input and output data between the program modules a data management system is used storing all actual data during the design iteration in an internal data base. With this kind of data handling the order of the modules in the design process can be rearranged easily, in addition they can work as stand-alones combined in a user specified manner as a design tool-kit.

4. Level: Design Program Libraries. The program libraries include the different physical models used during the design process. They form the kernel in which methods developed by different disciplines can be integrated as new modules to enhance the accuracy of the design code. One element of the libraries is the data management system (DMS) as an important tool for handling and manipulating design information. For using the DMS, the design engineer has only the task to add the DMS-calls (e.g. storing, retrieving, creating a new data base, saving a data base) to his new developed routine and to modify the input and output parts of the code. In this way the routine becomes a new module as part of the design program PrADO. Due to the data management system PrADO gets an open-end capability and a great flexibility with respect to the adaption to new applications.

PrADO - Analysis Models

With respect to the canard studies, the basic geometry (wing planform, span, body length, horizontal and vertical tail volume etc.) of the current A3XX configuration with dimensions according to Ref. 6 was frozen in the first step. Instead of the proposed elliptical fuselage cross section a circular cross section was assumed, leading to a 9-abreast upper-deck and a 10-abreast lower-deck layout. Hence, the canard was integrated into a geometrically fixed configuration. For the SCT studies, the Concorde shape was taken as geometric baseline with dimensions given in Ref. 6. However, a symmetric configuration with plane wing was assumed, opposite to the real Concorde.

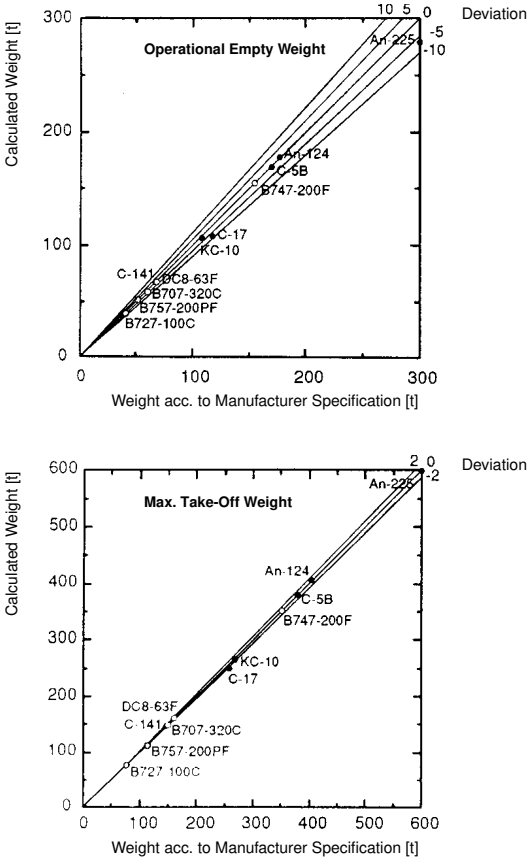

Fig. 3 Results obtained with PrADO (original version) for conventional transport aircraft.[1]

The aerodynamic analysis of the original PrADO version is based on lifting-surface theory, using engineering methods[7] in the transonic flow regime. This certainly leads to good results for conventional aircraft configurations, Fig. 3, but it is not suitable for the simulation of the aerodynamic interactions between canard, wing and tailplane, for instance. For this reason the higher-order panel code HISSS was implemented. A short description of the code is given in the following section.

In the canard studies the aerodynamic coefficients were calculated for 3 Mach numbers (M_∞ = 0.3, 0.6 and 0.85). Between the 3 Mach numbers, the aerodynamic characteristics were interpolated and kept constant below M_∞ = 0.3. Since both control devices, horizontal tail plane and canard, are used for triming, 9 different combinations of canard and tail plane angle were simulated to determine the interaction effects on the aerodynamic behavior. Friction drag is added according to the friction on a flat plate. In the transonic speed regime the semi-empirical methods for the estimation of non-linear aerodynamic effects of the original PrADO version were applied.

The aerodynamic simulation of the SCT comprises 6 Mach numbers (M_∞ = 0.3, 0.7, 0.9, 1.1, 1.3 and 1.5). An interpolation algorithm is used to calculate the aerodynamic coefficients between, according to Fig. 4, except for the lift-curve slope $\partial C_L / \partial \alpha$ in the transonic flow regime. In the

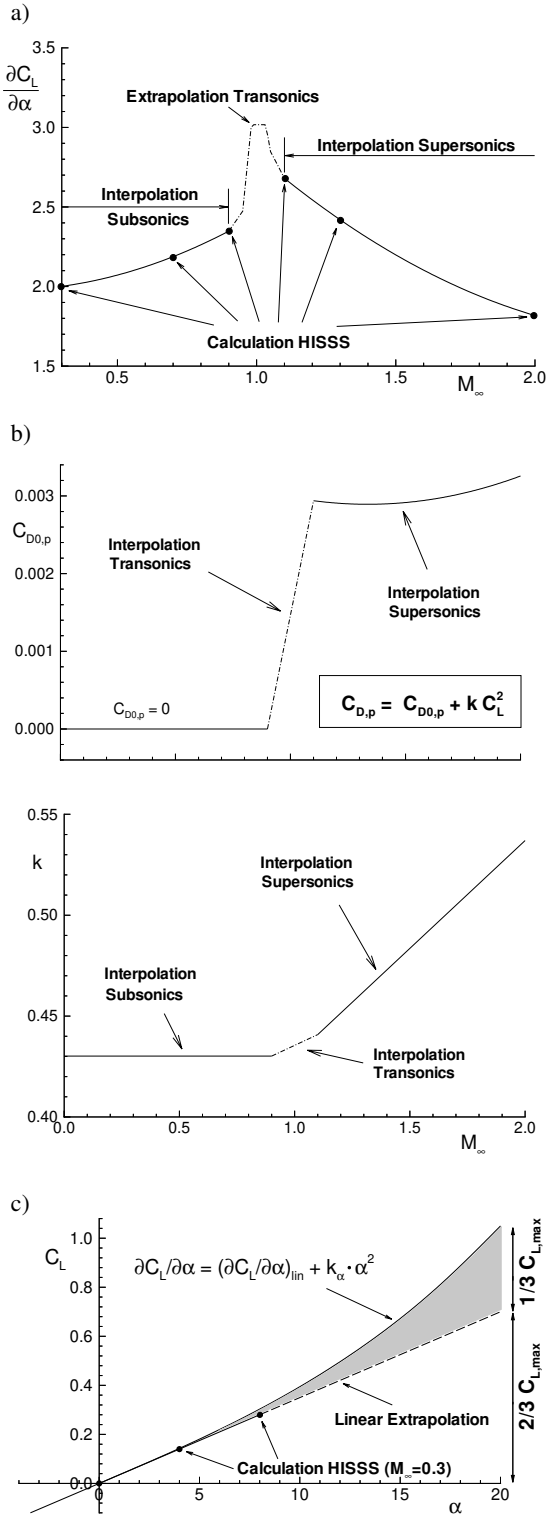

Fig. 4 Calculation of aerodynamic coefficients in PrADO for supersonic configurations:
a) lift-curve slope
b) pressure drag
c) max. lift coefficient.

range from $M_\infty = 0.9$ to 1.1 an extrapolation from the subsonic and the supersonic flow regime is applied, limiting the maximum value according to experimental data provided in Ref. 8. Due to the symmetry of the configuration with respect to the waterplane, the simplified formulation for a quadratic drag polar is used to determine the pressure drag. Based on experimental data[9] the maximum lift relevant for the take-off performance is assumed to occur at $\alpha = 20°$ and is provided to 1/3 by additional vortex lift due to leading-edge separation (Fig. 3 c). Non-linear lift effects are assumed to occur up from $\alpha = 4°$.[9]

In the following propulsion module thrust and fuel consumption characteristics of existing (e.g. CFM56-5) or projected engines (e.g. CRISP propfan) are available. Alternatively a scalable turboprop-, turbojet- or turbofan 'rubber engine' can be chosen, modeling the thermodynamic cycle for the calculation of thrust and fuel consumption. For the investigations a high bypass turbofan rubber engine with a bypass ratio of $\lambda = 6$ was chosen and validated using thrust and fuel consumption data of modern high thrust / high bypass ratio engines, provided by BMW Rolls-Royce AeroEngines. The new integrated engine model[5] for the SCT investigations also bases on the simulation of the thermodynamic cycle. It allows the simulation of a turbojet as well as turbofan engine, including afterburning for take-off and passing the sound barrier. In the present studies the turbojet engine was chosen.

The necessary maximum take-off thrust for the engine layout is determined according to FAR 25 by the highest of the following demands: Meeting the maximum take-off distance, minimum climb potential at cruise begin, in the second segment and during approach with one engine inoperative as well as the minimum landing climb potential to ensure safe wave-off after a baulked landing.

After the engine layout the mission is simulated in the flight performance module. A trimed mission of 14,200 km (7650 nm) with 656 passengers and no additional payload is prescribed in the canard analyses, assuming a cruise flight with $M_{\infty,cr} = 0.85 = \text{const.}$ and $C_{L,cr} = 0.5 = \text{const.}$ To determine the trim conditions an iterative algorithm was integrated, analyzing the relevant combinations of α, ε_{HTP} and ε_C which guarantee $C_L = C_{L,\,req}$ and $C_{M,\,C.G.} = 0$ at the lowest drag. Static stability $\partial C_M / \partial C_L \leq 0$ is not required, but the neutral point position along the mission is provided in the output data to determine whether the configuration is stable or not. The SCT mission is simulated untrimed for a range of 6000 km (3250 nm), $M_{\infty,cr} = 2.0 = \text{const.}$ and $C_{L,cr} = \text{const.}$, 140 passengers and no additional payload.

The design of the aircraft structure is based on a finite element method for wing and tailplane. These components are modeled with 2-knot beam elements having a multi-cell cross section. According to JAR / FAR regulations 3 critical load cases are taken into account for the dimensioning of the wing: Rolling on the runway at take-off, flight with maximum manoeuver load and maximum gust load. Additional load cases are analyzed for the layout of tailplane and canard. The canard is treated in the same way as the horizontal tail plane. For the calculation of the SCT wing, however, a semi-empirical model according to Ref. 10 was chosen. In both cases, canard and SCT analyses, a semi-empirical method is also used for the calculation of the fuselage structure,[11] which takes into into account structure loads coming from wing, tailplane and canard as well as the fuselage pressure difference under cruise conditions. The mass of the propulsion unit is determined according to Ref. 12, the landing gear mass as well as the masses of all systems, equipment and operational items are based on the WAATS program.[13]

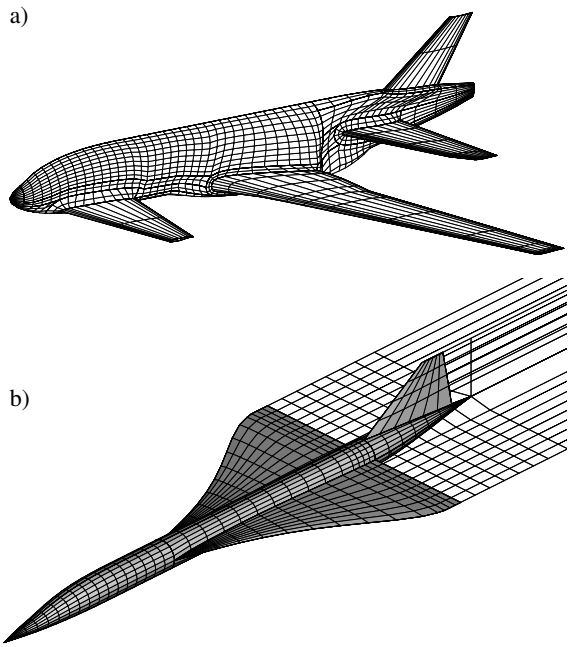

Fig. 5 PrADO-Grid results for an arbitrary three surface aircraft configuration (a) and an SCT (b).

In the final step of the iterative design process the tailplane is sized to guarantee sufficient control along the flight envelope from take-off to landing for the entire range of the center of gravity position.

The convergence of the iterative aircraft design process is checked at the end of the stability / control module. A design is considered converged, if the variation of prescribed relevant design parameters (e.g. maximum take-off thrust and take-off weight, mission fuel) falls below a presribed absolute and relative limit (e.g. maximum take-off weight variation below 0.5% and 50 kg). Larger variations of the chosen parameter lead to a return to the beginning of the design procedure. Finally, the converged design may be assessed based on a defined objective function, which is especially relevant for the control of the optimization algorithm.

HISSS - Code, Grid Generation and Validation

The panel code HISSS[4] is a higher-order singularity method for the solution of linear potential flow around arbitrary three-dimensional configurations at subsonic and supersonic speeds. Composite source / doublet panels are used on the surface of the configuration, the wake panels have a doublet distribution to carry downstream the vorticity generated over the surface of the configuration. The Kutta condition at trailing edges is fulfilled without Kutta panels.

The application of HISSS requires a panel grid consisting of the surface grid and wake networks. For this reason the grid generation routine PrADO-Grid was developed. PrADO-Grid provides suitable panelgrids for SCT, canard and conventional aircraft configurations based on the geometry information coming from the geometry module. In Fig. 5 examples for an SCT and canard configuration are given:

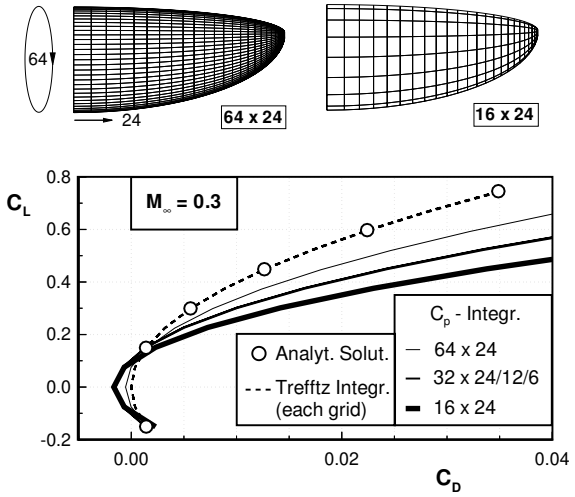

Fig. 6 Influence of grid fineness and method on drag calculation in HISSS.

Opposite to the SCT with an H-topology, the routine uses a C-H topology for conventional and canard configurations to guarantee regular grids in the intersection between fuselage and wing (tailplane, canard). HISSS also runs in the optimization mode of PrADO where strange designs may be proposed by the optimization algorithm, as shown in Fig. 5a. Hence, special importance was attached to the robustness of the grid generation method. Up to now, pylon, nacelle and engine are not modeled for the panel calculations. Furthermore, in the numerical simulation only one half of the configuration is calculated for reason of symmetry; sideslip conditions are not taken into account to reduce the numerical effort.

Detailed analyses of the influence of the grid fineness on the aerodynamic coefficients showed a strong dependency of the induced drag on the grid fineness if it is calculated via surface integration of the pressure coefficient, as illustrated in Fig. 6 for the elliptical wing with NACA-0012 profile. Even fine grids do not provide a proper result. However, the

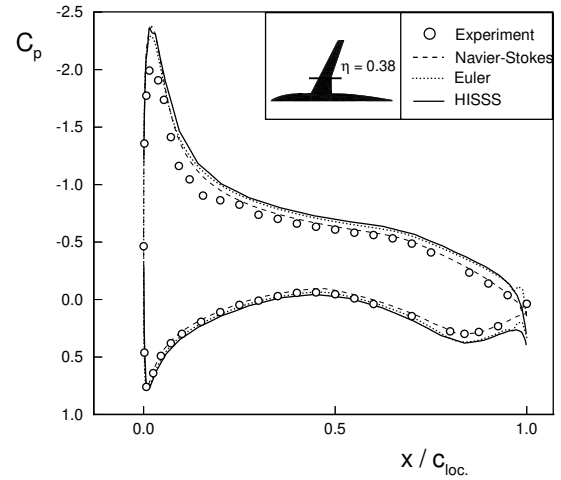

Fig. 7 HISSS validation using the ALVAST configuration ($M_\infty = 0.27$, $\alpha = 4°$).

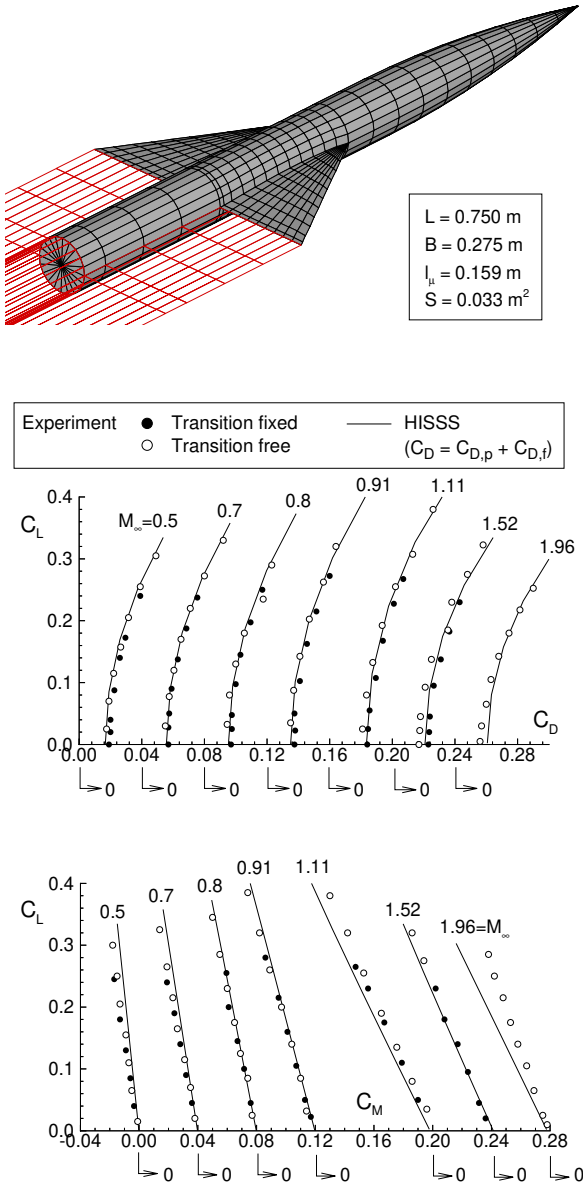

Fig. 8 HISSS validation for slender supersonic configurations.

influence of the grid fineness on lift and pitching moment coefficient is neglectable. To guarantee proper drag calculations even for coarse grids which have to be applied in the predesign studies to reduce iteration time, the drag coefficient is calculated based on the circulation distribution in spanwise direction and the downwash in the Trefftz plane. This method provides accurate drag coefficients almost independent of the fineness of the surface grid.

The validation of the panel code is illustrated exemplarily in Figs. 7 and 8. Figure 7 shows the wing surface pressure distribution of the ALVAST configuration for a typical subsonic testcase. The differences between the result of HISSS and the Euler code are small. However, viscous effects, such as the reduction of the rear loading due to the boundary layer influence on the effective camber of the profile cannot be predicted, neither from the panel code nor from the Euler method. The second example in Fig. 8 shows a comparison

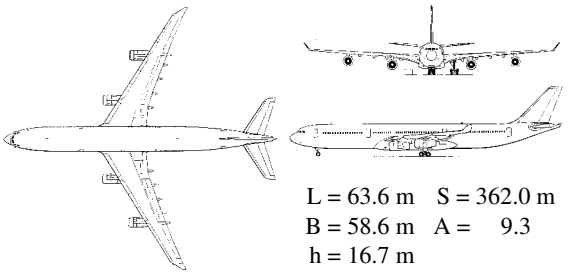

L = 63.6 m S = 362.0 m
B = 58.6 m A = 9.3
h = 16.7 m

Mission: 295 Pax $M_{\infty,cr}$ = 0.86
R = 12,500 km H = 10.01 km

Weights [t]:	Literature[6]	PrADO
Wing	n.a.	37.0
Fuselage	n.a.	25.4
Tailplane	n.a.	2.5
Land. Gear	n.a.	11.2
Engine	n.a.	20.5
Sys. & Acc.	n.a.	32.1
Operat. Empt.	128.8	128.7
Tot. Fuel	102.3	102.4
Max. Take-Off	258.0	258.0

Fig. 9 Redesign of A340-300 for calibration of PrADO.

between experimental results and HISSS for lift, drag and pitching moment of a slender configuration from $M_\infty = 0.5$ to $M_\infty = 1.96$. For comparison of the drag, friction drag was added to the HISSS results according to the friction on a flat plate in turbulent flow for windtunnel Reynolds numbers. The HISSS results compare well with the experimental data along the entire Mach number range.

Results

1. Megaliner Canard Configuration

Before the design of the Megaliner configuration with and without canard, PrADO was calibrated on the basis of a redesign of the A340-300 as an existing wide body. The configuration, mission data and results of the calibration are given in Fig. 9. The differences concerning operational empty weight, fuel weight and maximum take-off weight are marginal.

In a second step, a Megaliner configuration corresponding to the geometry, performance and mission data of the A3XX-200 was designed. For the cruise flight at $M_{\infty,cr}$ = 0.85 a lift coefficient of $C_{L,cr} = 0.5$ was chosen. The required mission data and dimensions as well as the configuration and weight breakdown of the design are given in Fig. 10 and are compared with published data.[6] With respect to the relevant weights the differences between PrADO design and predicted weights in literature are below 6 %. This is comparable to the order of accuracy which was obtained with the original version of PrADO, see Fig. 3.

In the final step, 3 canard configurations with different canard span, B_C = 20 m, 30 m and 40 m were designed, based on the A3XX-200 layout. The geometric characteristics

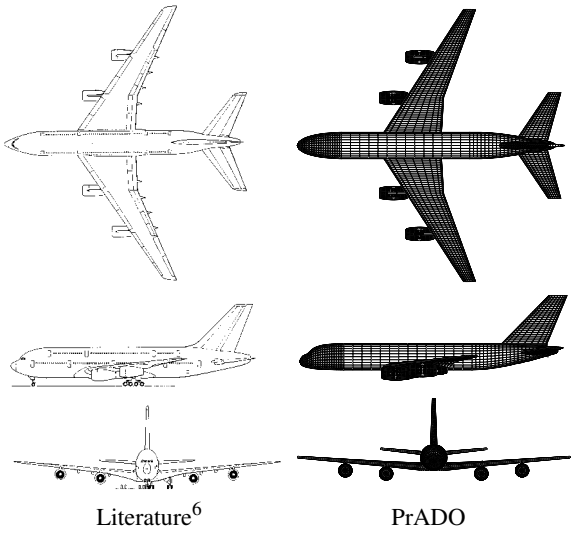

Literature[6] PrADO

Dimensions: L = 70.8 m S = 774.0 m
B = 79.0 m A = 8.1
h = 24.3 m

Mission: 656 Pax $M_{\infty,cr}$ = 0.85
R = 14,200 km $C_{L,cr}$ = 0.5

Weights [t]:	Literature[6]	PrADO
Wing	n.a.	89.7
Fuselage	n.a.	52.6
Tailplane	n.a.	8.5
Land. Gear	n.a.	27.0
Engine	n.a.	31.4
Sys. & Acc.	n.a.	69.0
Operat. Empt.	286.0	278.2
Tot. Fuel	237.3	225.1
Max. Take-Off	583.0	562.6

Fig. 10 Design of A3XX-200 with PrADO.

of the canards as well as the planform shape of the configurations are given in Fig. 11a. To illustrate the fineness of the grids used in the panel calculations within the design process, the surface grid of the configuration with B_C = 40 m is given in Fig. 11b. The result of the integrated predesign is summarized in Fig. 12 and compared with the A3XX-200 design without canard. The unexpected result is that in spite of the lifting control device each canard configuration shows an aerodynamic efficiency L / D_{cr} which is smaller compared to that of the baseline design without canard. The reduction of the induced drag, based on a triming with the lifting canard, is overcompensated by the additional friction drag of the canard, since minimum drag and induced drag are of the same order of magnitude. The L / D_{cr} is reduced with increasing span of the canard configuration.

Configuration:	canard span [m]	0.	20.	30.	40.
Aerodynamics:	minimum drag	0.0134	0.0140	0.0146	0.0154
	induced drag	0.0115	0.0110	0.0113	0.0107
	tot. drag	0.0249	0.0250	0.0259	0.0261
	lift	0.5	0.5	0.5	0.5
	L / D	20.1	20.0	19.3	19.2
Weights:	canard [t]	0.0	2.1	5.1	10.0
	operat. empty [t]	278.2	281.2	288.2	295.9
	tot. fuel [t]	225.1	227.8	244.6	252.8
	max. take-off [t]	562.6	568.3	592.1	597.6
Stability:	x-pos. center of gravity [m]	34.75	34.40	33.98	33.43
	x-pos. neutral point [m]	38.52	36.96	34.72	31.97

Fig. 12 Preliminary results of the canard analyses.

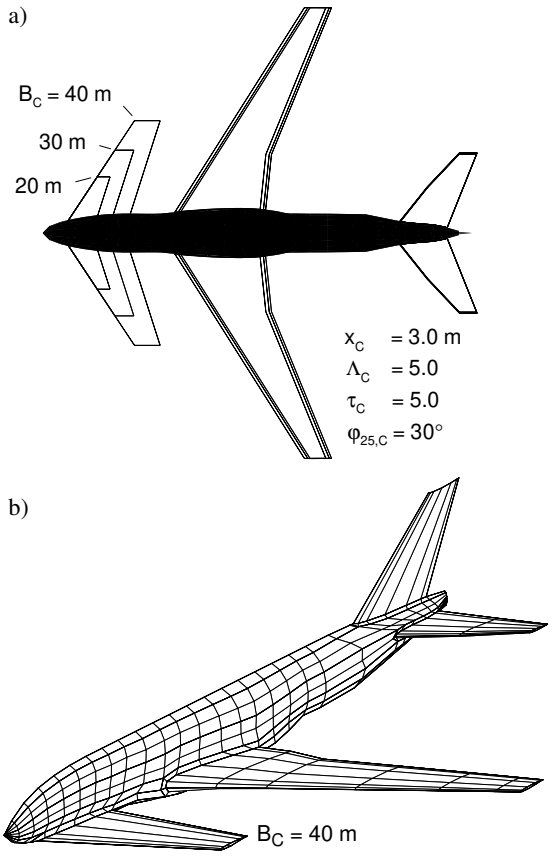

Fig. 11 Investigated canard configurations (a) and panelgrid for the HISSS calculations (b).

In addition, the weight analysis shows an increase of the operational empty weight due to the introduction of the canard. This finally leads to a lower cruise altitude which increases the drag at fixed lift due to a higher dynamic pressure. With respect to the static stability a neutral point shift to the nose occurs with increasing canard span and the configuration with B_C = 40 m is not static stable, the neutral point is located in front of the center of gravity.

2. SCT Analysis

In Fig. 13 the resulting drag polar of the concorde redesign is shown and compared with experimental data.[9] Close to the design point both results compare very well. The resulting operational empty weight, maximum take-off weight and the mass breakdown is given in Fig. 14. Compared with the data published in literature[14] the operational empty weight is predicted approximately 16 % higher. The mass breakdown indicates significant discrepancies between predicted and published fuselage and system weights.[15]

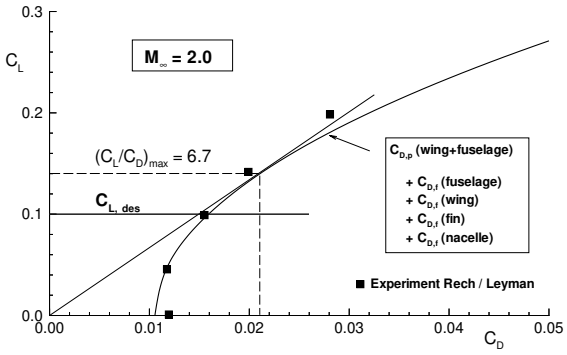

Fig. 13 Drag polar of redesigned Concorde at M_∞ = 2.0 (untrimed).

	Literature[14,15]	PrADO
Max. Take-Off	176.5 t	186.8 t
Operat. Empty	78.3 t	90.9 t
Service	4.5 %	4.2 %
Accomodation	6.8 %	6.3 %
Systems	13.7 %	8.0 %
Landing Gear	9.1 %	7.9 %
Fuselage	14.9 %	24.0 %
Tailplane	4.1 %	2.2 %
Wing	17.3 %	17.8 %
Inlet	6.4 %	6.4 %
Nozzle	6.4 %	6.4 %
Engine	16.8 %	16.8 %

Fig. 14 Weight breakdown of redesigned Concorde.

Summary

In the present paper the improvement of an integrated aircraft predesign code and its application to future aircraft concepts is reported. For the simulation of a Megaliner canard configuration as well as a supersonic commercial transport aircraft (SCT) the predesign code PrADO was extended by the higher-order panel method HISSS. The improvement of the aerodynamic model allows the simulation of interference effects between wing, tailplane and canard as well as the extension of the simulated flight regime to supersonic speeds.

The application of the calibrated predesign code to a Megaliner configuration leads to differences between published and predicted design weights below 6 %. Preliminary results of the simulation of a canard configuration show that a canard may not automatically increase the aerodynamic efficiency L / D. For canard configurations with a span between 20 m and 40 m and a cruise lift coefficient of $C_{L,cr}$ = 0.5 the canard integration reduces the L / D_{cr}. A reduction of the induced drag is overcompensated by an increase of the minimum drag due to additional friction drag of the canard.

The SCT design studies also provide converged solutions, however, a redesign of the Concorde shows significant discrepancies with respect to the operational empty weight, fields for future investigations.

Acknowledgements

The authors thank L. Fornasier, Daimler-Benz Aerospace (DASA), Munich, for providing the panel code HISSS and his support. W. Heinze of the Institute of Aircraft Design and Structure Mechanics, TU Brunswick, is gratefully acknowledged for the helpful discussions with respect to the application of PrADO and general aspects of the integrated predesign. Further acknowledgement is given to J. Stilla, BMW Rolls-Royce AeroEngines, Berlin, for providing the authors with engine data for validation purpose and F. Deidewig, Institute of Propulsion Technology, DLR Cologne for his SCT engine model.

References

1. Kossira, H.; Heinze, W.; "Untersuchung über die Auslegungsgrenzen zukünftiger Transportflugzeuge", DGLR-Jahrbuch I (1990), pp. 35-49.
2. Hertel, J.; Albers, M.; "The Impact of Engine and Aircraft Design Interrelations on DOC and its Application to Engine Design Optimization", AIAA Paper 93-3930, 1993.
3. Bardenhagen, A.; Kossira, H.; Heinze, W.; "Interdisciplinary Design of Modern Hypersonic Waveriders Using the Integrated Program PrADO-Hy", ICAS Paper 94-1.4.1, 19th International Council of the Aeronautical Sciences, 1994.
4. Fornasier, L.; "HISSS - A Higher-Order Subsonic/Supersonic Singularity Method for Calculating Linearized Potential Flow", AIAA Paper 84-1646, 1984.
5. Deidewig, F.; "Ermittlungen der Schadstoffemissionen im Unter- und Überschallflug", DLR-FB 98-10, DLR Köln, 1998.
6. Jane's All The World's Aircraft, 1997-98.
7. Hoerner, S.F.; "Fluid-Dynamic Drag", Hoerner Fluid Dynamics, New York, 1965.
8. Schlichting, H.; Truckenbrodt, E.; "Aerodynamik des Flugzeugs", 2. Bd., Springer-Verlag, Berlin, 1969.
9. Rech, J.; Leyman, C.S.; "A Case Study by Aerospatiale and British Aerospace on the Concorde", AIAA Professional Study Series.
10. Nicolai, L.M.; "Fundamentals of Aircraft Design", University of Dayton.
11. Simpson, D.M.; "Fuselage Structure Weight Prediction", SAWE Paper 981, 1973.
12. Waters, M.H.; Schairer, E.T.; "Analysis of Turbofan Propulsion System Weight and Dimensions", NASA TM-73195, 1977.
13. Glatt, C.R.; "WAATS - A Computer Program for Weight Analysis of Advanced Transportation Systems", NASA CR-2420, 1974.
14. Barfield, N.; "Aerospatiale/BAC Concorde", Aircraft Profiles, Profile Publications, Coburg House, 1973.
15. Mizuno, H.; Hagiwara, S.; Hanai, T.; Takami, H.; "Feasibility Study on the Second Generation SST", AIAA Paper 91-3104, 1991.